International Journal of Early Childhood Special Education (INT-JECSE)
DOI:10.9756/INTJECSE/V14I5.638 ISSN: 1308-5581 Vol 14, Issue 05 2022

AIR POLLUTION DETECTION FROM SKY IMAGES WITH DEEP CLASSIFIERS

R.Udaya Bharathi [1], Dr. M.Seshashayee [2]
1. Research Scholar, Department of Computer Science, GITAM (Deemed to be University), Vishakhapatnam, Andhra Pradesh, India. Emailid:udai158@gmail.com.
2. Assistant Professor, Department of Computer Science, GITAM (Deemed to be University), Vishakhapatnam, Andhra Pradesh, India. Emailid:smaruvada@gitam.edu.

Abstract:
People who are not able to rely on the daily declarations of air pollution levels by organizations like municipalities may find it useful to use cameras to detect the degree of pollution in an image. The proposed technique uses smart phone camera feature for estimating local air pollution . A large collection of pictures are taken throughout the city of Tehran. Next, a pair of strategies are used for determining how severe air pollution really is. The photos are first pre-processed, and then features are extracted using the Gabor transform. Last but not least, two simple categorization strategies are used to estimate and forecast the air pollution level. The second approach takes a picture of the sky as input and outputs a measure of air pollution based on its quality. This is accomplished by a Convolutional Neural Network (CNN). A suggested approach has been tested in a few studies, based on the findings, it can be concluded that the suggested technique detects air pollution levels with a degree of accuracy that is satisfactory. The 90% plus percentage accuracy attained by our deep classifier is an improvement of around 10 percentage points above the performance of standard feature extraction and classification approaches.

"Keywords: Convolution Neural Network. Gabor transform, Air pollution, image processing

Introduction

When harmful substances, such as particles and biological molecules, are released into the atmosphere, it is referred to as air pollution. Diseases, allergies, and even death may be caused by polluted air. Air pollution has become a major concern in many industrialized countries. Breathing filthy air may increase your risk of developing diseases, allergies, and even death. It might also have serious consequences for other kinds of life, including as animals and food crops, as well as for the natural and artificial ecosystems. Both human activities and natural events may contribute to air pollution. For example, when individuals go to work each day by driving vehicles and using other petroleum-based products as a source of energy, they contribute to air pollution. Fossil fuels are needed in the production of electricity. Since pollution has increased globally, global temperatures have risen.

According to the WHO, air pollution is directly responsible for approximately 3 million deaths annually. Exposure to air pollution has been established as a key factor to respiratory and cardiovascular illnesses [1].

Airborne Particulate Matter (PM), particularly microscopic particles with diameters less than 2.5 m (PM2.5), has an outsized influence on human health compared to other air pollutants [2, 3]. There are a variety of techniques available for estimating PM mass concentrations in the air. Some of the more methods are black smoke measuring etc. All of these methods need sophisticated equipment that most people just cannot afford. A simple, quick and economical way to detect PM in air have the potential to raise public awareness, inform patients with respiratory diseases to take essential preventive steps, and deliver local air quality data that are not otherwise available.

Air pollutants are components in the air that may have bad consequences on human being and the environment. Materials may take the shape of solid particles, liquid droplets, or gas molecules. A pollutant may have either a natural or an artificial origin. Primary and secondary pollutants are two types of pollution. Most primary pollutants, like volcanic ash, are byproducts of some other activity. Carbon monoxide gas and sulphur dioxide from cars and trucks are primary pollutants. Non-primary pollutants are not released into the atmosphere in this way. Instead, they emerge in the atmosphere as the result of interactions between basic contaminants. One well-known secondary contaminant is ozone at ground level. Primary pollutants are those that are released directly, whereas secondary pollutants are those that are generated when primary pollutants react with one another.

Air pollution, on the other hand, poses serious health risks to locals. Some parts of the nation use a wide variety of strategies to deal with this issue. Many countries, like China, employ plants in buildings and towers to remove CO_2 from the air, while many others develop and produce electrical automobiles to help keep the air clean. People should be aware of how severe the air pollution is where they live.

Fig 1. Sample images from database on two different days

The dataset covering many days in Tehran was gathered. Images from two days in the same location but with drastically varying levels of air pollution are shown in Fig. 1.

Two techniques are suggested for using satellite imagery to gauge pollution levels in the atmosphere. First method involves feature extraction in the shallow version which utilizes a Gabor filter, and for modelling a pair of classification algorithms is used. The second method involves classifying the data using a convolution neural network (CNN) as a deep architecture.

Related Works:

Prenatal development may be impacted by air pollution. The MAPSS (Maternal Air Pollution in Southern Sweden) partner includes transparent data considering private locations, a birth library, and an ultrasonography informative index covering around 48,000 pregnancies. Delivery weight and head frame were evaluated after birth, and the effects of air pollution on these parameters were evaluated in [5] with direct backslides for the aforementioned endpoints.This study looked at the seemingly insignificant effects of air pollution on birth weight, length of gestation, and overall fetal development [5].

Schultza et al. [6] analyze hypersensitive sickness association with provincial and restricted assessments of air pollution. This research set out to assess the regularity of three new sensitive disease outcomes in adults: sensitivity, asthma, and wheezing in relation to breathing in fine particulate matter (PM2.5), air taint from vehicles, and air pollution from electrical currents.

Exposure to natural light from the sun provides more than 90% of the vitamin D the human body needs [7]. Pollution in the environment alters the protective effects of vitamin D. When air pollutants absorb and re-emit UVB rays from the sun, they diminish the sun's ability to provide enough sunlight for vitamin D production [8].Thus, air pollution levels have a determining function in the improvement of lack of vitamin D. As a result, hypovitaminosis D is hypothesized to be an atypical effect of air pollution in very polluted places that also get significant exposure to sunlight.

Air pollution levels are difficult to predict. Based on an analysis of several outdoor photographs taken in Beijing, Shanghai, and Phoenix, the study [9] suggested a method to quantify PM air pollution. In this research, six components were eliminated from the photographs. They were used in conjunction with things like the sun's position, the time of day, geographical data, and meteorological trends to predict the PM2.5 file. In [10], we take a look at how satellite images are processed and where exactly air pollution is located.

Fig 2. Sample images of different views in the database

Gabor filter:
The Contourlet Transform [11], auxiliary models [12], and the Gabor channel [13] are just a few examples of the many mathematical transformations available for stripping surfaces from images. Gabor channels are instantaneous channels used for area detection and edge extraction in digital images. The visual system of a person is quite similar to the visual system shown by Gabor channels, particularly with regard to the repetition and continuity of images. The Gabor channel is especially useful for surface depiction and division. A 2D Gabor channel is a Gaussian capacity piece in spacetime that has been modulated by a planar sinusoidal wave.
Ability to use Gabor filters may be a marker for key cells in the mammalian visual cortex [13]. Thus, it is acknowledged that assessing images using Gabor channels is analogous to how humans see the world. The driving response may be described as a Gaussian expansion of a sinusoidal wave (a plane wave for 2D Gabor channels). For a Gabor channel, the drive response's Fourier difference is the convolution of the channel's consonant capacity and Gaussian ability, thanks to the channel's enhanced convolution feature (Convolution hypothesis). Both actual and fantasy elements in the river are working to maintain a steady flow.
Using a large number of Gabor channels with a variety of frequencies and orientations might be useful for eliminating background clutter in an image. Discrete-time Gabor channels with two layers are supplied by the following equations:

$$“G_c[i,j] = Be^{\frac{(i^2+j^2)}{2\sigma^2}}\cos\left(2\pi f(icos\theta + jsin\theta)\right)$$

$$G_s[i,j] = Ce^{\frac{(i^2+j^2)}{2\sigma^2}}\sin\left(2\pi f(icos\theta + jsin\theta)\right)$$

In where B and C are unknown normalization constants. 2D Gabor filters find widespread use in many areas of image processing, particularly in the realm of feature extraction used for texture analysis and segmentation. A texture's search frequency is specified by f. We may search for texture with a certain orientation by adjusting. By morphing, we modify the cause, or the size of the image area being assessed.

PROPOSED METHOD:
The initial strategy relied on simple classifications made using shallow machine learning methods. The second strategy makes use of a deep modelling architecture.

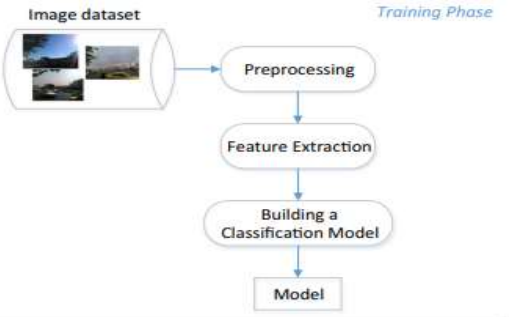

Fig 3. Block diagram for proposed method1 training phase

Data acquisition:
To do this, we will need access to a large collection of images taken on days with varied levels of air pollution. In this regard, we gathered photos from five areas in Tehran from 18 October 2016 to 31 May 2017 using a 5-M pixel camera. The camera was not positioned permanently. However, we aimed to gather images from certain points in the streets. Images may therefore have a slightly varied horizon line and range of vision. These regions were picked as indicative of metropolitan settings, with significant levels of air pollution owing to the large numbers of automobiles there. The Municipality of Tehran publishes its daily report of air pollution readings in these locations at 8 AM and 11 AM. Some instances of these views during a day are illustrated in Fig. 2. From the website www.air.tehran.ir, we were able to acquire data on the air pollution levels of various places on different days, which we subsequently overlaid over the relevant photographs. Fig. 3 shows the location of stations for monitoring of air pollution in City of Tehran on 15 November 2017.
The Municipality of Tehran evaluated air quality on a scale from "excellent" to "good," "lightly polluted," "moderately polluted," and "heavily polluted." Which is shown in Table1. Municipality on each day and for each site announces the air pollution level from the five prescribed level. Therefore, for each example image we

labelled the pictures from this collection according on the announcement of Municipality for each area. The Municipality distributes the information on each day for select designated places in Tehran.
482 images in the dataset have been utilised. Table 4 shows the number of pictures taken at various degrees of air pollution.

"Air Quality level	Excellent	Good	Lightly polluted	Moderately polluted	Heavily pollutes
Number of images	100	256	88	38	0

Table 1: Number of instances in class in the collected dataset

First method
There are several processes inside each of the two main phases of our method for evaluating air pollution. Figure 3 depicts the suggested method during its training phase, whereas Figure 4 depicts its testing phase.

Pre-processing:
For each picture, the sky takes up around half the frame. When trying to predict how polluted the air will be, the sky is the best place to look. Because buildings come in a wide variety of shapes, sizes, colours, and textures, predicting pollution levels only by looking at pictures of them is not possible. When making an accurate prediction of air pollution, we crop a rectangle to exclude everything except the sky. All the training photos go through this procedure throughout the training phase.
Feature extraction:
All photos used throughout the training and testing stages undergo feature extraction. The Gabor transform to pull out the underlying texture in photos. Image texture may be extracted using the aforementioned transform thanks to the varying hues of pollution in various parts of the picture.
The next step is to take the filtered photos and draw out the feature vectors. To this end, we perform statistical moment calculations on the filtered pictures before constructing the model (classifier). The moments of statistics we will be covering are the mean, variance, kurtosis, standard deviation, and skewness.
Classification:
"Commonly used techniques for classification include Random Forest (RF) and K-Nearest Neighbor (KNN)."
Second method:
Three convolutional layers, two scaling layers, and two fully linked layers make up the proposed CNN's total of seven layers. Corrected direct units (ReLUs) are used to do a linear transformation followed by a nonlinear guidance in each layer in order to speed up the learning processes. Exposing the first two levels to neigh bring response standards improves conjecture. Max pooling is used on all convolutional layers except the third to achieve translational invariance. Warped RGB picture patches of size 200 200 are sent into the network as input. In Fig. 4, we see the network's elaborate framework laid out in full.

Fig 4. The architecture of the CNN in the second proposed method2

Experimental results:
Evaluation of first proposed method:
Ten-fold cross-validation is used to validate test results, and the mean Area Under Curve (AUC), Accuracy, F1 measure, Precision, and Recall are calculated across categories. Summing the values in the first slanting yields the Total True Positive (TP) obtained from evaluating a model against test data shown in Table 5. Class x equals the sum of column x. (without the primary askew). The number of lines in class x is equal to the bogus negative (FN) for that class (without the primary askew).

Method description	Accuracy	F1	Precision	Recall
100 tress and depth 5	0.922	0.86	0.92	0.82
200 tress and depth 5	0.922	0.83	0.92	0.82
300 tress and depth 5	0.82	0.83	0.93	0.82

Feature selection & 100 tress and depth 5	0.93	0.79	0.87	0.86
Feature selection & 200 tress and depth 5	0.93	0.74	0.83	0.86
Feature selection & 300 tress and depth 5	0.93	0.75	0.75	0.86

Table 2: Classification accuracy of the first proposed method employing Random Forest method on prediction the air pollution level

In this evaluation, we handle a 5-class order problem for which the exactness of irregular speculating with no exhibiting is (100/5) =20 percent. The next tables present precise findings that illustrate the amount more feasible a model would than irregular "guess.

$Accuracy = (TP + TN)/(TP + FP + FN + TN)$ (3)

$Precision = TP/(TP + FP)$ (4)

$Recall = TP/(TP + FN)$ (5)

$F1 = 2X(Recall\ X\ Precision)/(Recall + Precision)$ (6)

If we employ the whole available time in the random forest technique, we improve accuracy to 90% plus. Inaccuracy increases after feature selection.

Method description	Accuracy	F1	Precision	Recall
K = 1	0.88	0.84	0.87	0.88
K = 15	0.88	0.84	0.88	0.88
K = 20	0.88	0.84	0.88	0.88
Feature selection & k=10	0.88	0.88	0.87	0.88
Feature selection & k=15	0.89	0.86	0.86	0.89
Feature selection & k=20	0.89	0.86	0.86	0.89

Table 3: Classification accuracy of the first proposed method employing KNN method on prediction the air pollution level

Evaluation of second proposed method:

Table 4displays the results of testing many distinct CNN models on the accuracy of their respective location predictions. The number of layers, layer grouping, convolutional channel size, scaling factor, and number of element mappings are all customizable. Table 4indicates the strongest produced result, which is a good thing.

The results of Table 4 show that the development of Line 8 yielded the highest precision. Even while the scale layers do not have a major impact on the display, the number of element mappings does. Similarly, it makes no difference how big the convolutional channel is. Tables 2, 3, and 4 reveal that a fundamental CNN structure achieves good accuracy than shallow classifiers like KNN and irregular forests.

No.	Layers	Accuracy
1	C(10)(5)-S(2)- C(10)(7)-S(2)- C(10)(5)-S(2)- C(4)(7)	86.25%
2	C(10)(5)-S(2)- C(10)(7)-S(2)- C(10)(5)-S(2)- C(2)(7)	78.75%
3	C(10)(5)-S(2)- C(10)(7)-S(2)- C(10)(5)-S(2)- C(10)(7)	56.88%
4	C(10)(5)-S(2)- C(10)(7)-S(2)- C(10)(5)-S(2)	88.13%
5	C(4)(5)-S(2)- C(6)(7)-S(2)- C(10)(5)-S(2)	89.75%
6	C(4)(5)-S(2)- C(6)(5)-S(2)- C(10)(5)	84.50%
7	C(4)(5)-S(2)- C(6)(5)-S(2)- C(7)(5)	82.25%
8	C(6)(5)-S(2)- C(6)(5)-S(2)- C(6)(5)	93.38%
9	C(6)(5)-S(2)- C(6)(5)-S(2)- C(5)(5)	84.75%

10	C(6)(5)-S(2)- C(6)(5)-S(2)- C(4)(5)	88.25%

Table 4: Classification accuracy of the second proposed method (CNN) on prediction the air pollution level

Conclusion:

Airborne particles provide a unique visual aspect to captured photographs. Using various filters and transformations, we may determine an image's texture. Utilizing the Gabor channel for include extraction and the KNN and Random Forest order computations for showing, this research is possibly the earliest attempt to end user to measure air pollution from a picture. In the second technique, the crude photos are transmitted to a CNN for order. The results of certain tests meant to examine the suggested systems have been presented. In this study, a coherent CNN framework is shown. Eventually, the output of the convolutional layer may be sent into a layer with optional enactment capabilities like Re Lu. It is possible to acquire superior findings and avoid over fitting by employing the dropout strategy.

As an end, we may declare that the degree of air pollution can be expected from a picture with reasonable certainty. By and by, in the event that we wish to assess air contamination with more prominent accuracy, with additional photographs from distinct locations on various days with altering amounts of air contamination is critical. It features photographs obtained using a special camera and a broad view on the city.

REFERENCES:

[1]. Mousavi SE, Heydarpour P, Reis J, Amiri M, Sahraian MA (2017) Multiple sclerosis and air pollution exposure: mechanisms toward brain autoimmunity. Med Hypotheses 100:23–30. https://doi.org/10. 1016/j.mehy.2017.01.003

[2]. Narasimhan SG, Nayar SK (2002) Vision and the atmosphere. Int J Comput Vis 48(3):233–254. https://doi.org/10.1023/A: 1016328200723

[3]. Anderson JO, Thundiyil JG, Stolbach A (2012) Clearing the air: a review of the effects of particulate matter air pollution on human health. J Med Toxicol 8(2):166–175. https://doi.org/10.1007/s13181-011-0203-1

[4]. Macias ES, Husar RB (1976) Atmospheric particulate mass measurement with beta attenuation mass monitor. Environ SciTechnol 10(9):904– 907. https://doi.org/10.1021/es60120a015

[5]. Anderson TL, Ogren JA (1998) Determining aerosol radiative properties using the TSI 3563 integrating nephelometer. Aerosol SciTechnol 29(1):57–69. https://doi.org/10.1080/02786829808965551

[5]. Malmqvista E, Liewb Z, Källéna K, Rignell-Hydboma A, Rittnera R, Rylandera L, Ritzb B (2017) Fetal growth and air pollution - a study on ultrasound and birth measures. Environ Res 152:73–80. https:// doi.org/10.1016/j.envres.2016.09.017

[6]. Schultza AA, Schauerb JJ, Malecki KMC (2017) Allergic disease associations with regional and localized estimates of air pollution. Environ Res 155:77–85. https://doi.org/10.1016/j.envres.2017.01.039

[7]. Barrea L, Savastano S, Di Somma C, Savanelli M, Nappi F, Albanese L, Orio F, Colao A (2016) Low serum vitamin D-status, air pollution and obesity: A dangerous liaison. Rev EndocrMetabDisord. https:// doi.org/10.1007/s11154-016-9388-6

[8]. Wacker M, Holick MF (2013) Sunlight and vitamin D: a global perspective for health. Dermato-endocrinology 5(1):51–108. https://doi.org/ 10.4161/derm.24494

[9]. Liu C, Tsow F, Zou Y, Tao N (2016) Particle pollution estimation based on image analysis. PLoS One 11(2):e0145955. https://doi.org/10. 1371/journal.pone.0145955

[10]. Prochazka A, et al (2000) Satellite image processing and air pollution detection. ICASSP '00 proceedings of the acoustics, speech, and signal processing, 2000.

[11]. Sajedi H, Jamzad M (2010) CBS: Contourlet-Based Steganalysis Method. Journal of Signal Processing Systems 61(3):367–373

[12]. Razavi F, Sajedi H, Shiri ME (2016) Integration of Color and Uniform Interlaced Derivative Pattern Features for Object Tracking. IET Image Processing 10(2):1–10

[13]. Marčelja S (1980) Mathematical description of the responses of simple cortical cells. J Opt Soc Am 70(11):1297–1300. https://doi.org/10. 1364/JOSA.70.001297

[14]. Fogel I, Sagi D (1989) Gabor filters as texture discriminator. BiolCybern 61(2):103–113